

## RESEARCH ARTICLE

# Dynamic Contact Characteristics Analysis of Heavy-duty Track Rollers

B.J. Yan\*, Z.H. Zhang, H.Q. Zhang, W.J. Zhang, Z.D. Zhao, T. Yang

School of Mechanical Engineering, Taiyuan University of Science and Technology, 030024 Taiyuan, China

**ABSTRACT** - As an important component of the crawler walking device, the track roller needs to withstand strong impact and is prone to failure, which can lead to serious economic losses. This paper focuses on the track roller of the spreader as the research subject and investigates the dynamic contact characteristics between the track roller and the track plate. Using RecurDyn software, a virtual prototype model of the crawler walking device is established to analyze the variation in a vertical dynamic load of the track roller under different working conditions. Simultaneously, a finite element model of the contact between the track roller and the track plate is developed using Ansys Workbench, and its accuracy is verified using Hertz contact theory. Finally, the study discusses various influencing factors on the contact characteristics, including load, curvature of the contacting bodies, and material yield strength. The results indicate that the track rollers experience the highest dynamic load when climbing a slope, reaching a maximum load of 1191.44 kN. Moreover, the maximum contact stress is 1750.4 MPa, and the maximum Mises stress is 921.34 MPa during this operation. Importantly, when the load reaches 1218 kN, the maximum Mises stress of the track roller is 930.2 MPa, which may lead to roller failure after prolonged use. These findings provide valuable insights for the design and optimization of heavy-duty track rollers and offer significant assistance for various tracked vehicles.

## ARTICLE HISTORY

Received : 16<sup>th</sup> Nov. 2023

Revised : 23<sup>rd</sup> Jan. 2024

Accepted : 29<sup>th</sup> Feb. 2024

Published : 20<sup>th</sup> Mar. 2024

## KEYWORDS

Spreader

Track roller

Hertz theory

Finite element method

Contact characteristic

## 1.0 INTRODUCTION

With the further expansion of mineral resources exploitation, the spreader has been widely used for the mining process of various large-scale mines (coal mines, non-coal mines) [1,2]. It is mainly composed of a crawler walking device, slewing platform, discharging carrier, receiving arm, balancing arm and discharging arm, which is shown in Figure 1, Performing on-site work as shown in Figure 2. Due to its advantages of low ground pressure, high traction, and strong off-road capability [3,4], the crawler walking device is often used in the spreader. As one of the key parts of the crawler walking device, the track rollers support the weight of the whole machine, they roll on the track chain link or track guide plate to prevent the track from slipping laterally. Most previous designs of the track roller are only based on tradition and experience, which makes it easy to make it fail after a period of usage as shown in Figure 3. This will seriously influence the working safety and efficiency of the whole vehicle. More importantly, if the spreader stops working, it will bring serious economic losses to the enterprise. Therefore, it is of great significance to study the load distribution law and stress characteristics of the track roller.

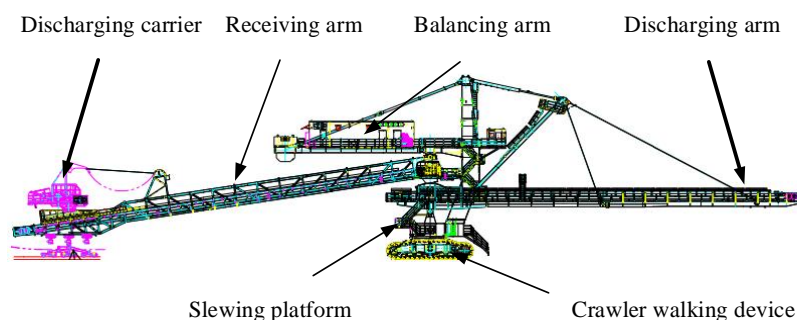


Figure 1. Structure diagram of the spreader



Figure 2. The fieldwork of the spreader



Figure 3. Failure diagram of track roller

In order to solve contact problems of two different elastic bodies, classical Hertz theory has often been used since Heinrich Hertz published the contact theory in 1881 [5]. For example, Yan et al. [6] proved that Hertz's theory is applicable to the rail-wheel contact problem. Tao [7] found that Hertz's theory could solve the normal contact problem of wheel wear well. Tian et al. [8] studied the static contact characteristics between the track roller and track plate and optimized the mathematical model of Hertz contact theory by using a genetic algorithm. Afterward, with the development of computer technology, the finite element method has been also widely used by researchers to investigate contact problems. For example, Aalami [9] used the finite element method to study the wheel-rail contact problem and discussed the stress distribution in wheel-rail contact. Arsla [10] discussed the basic method of solving the rail-wheel contact problem by using the finite element analysis method and introduced the steps of the solution. Sen [11] used the finite element method to study the fatigue life and parameter effects of UIC60 rail AT weld under vertical load. In order to better deal with the contact, many scholars have also adopted a combination of the Hertz theory and finite element. Yan et al. [12] established a mathematical model and finite element model of the track roller and plate and analyzed the influence of geometric parameters on the contact stress. Arsić et al. [13] obtained the surface contact stress of the track roller by using Hertz theory and finite element analysis, and the results showed that the failure of the track roller was mainly caused by "design defects" and "manufacturing defects". Sirata [14] used the analytical method and finite element simulation method to study the contact problem of rail wheels in the normal and tangential categories, in which the analysis method assumed elliptical contact patches based on Hertz's theory.

In recent years, multi-body dynamics software has provided convenience for solving the dynamics of tracked vehicles. For example, Pei [15] used RecurDyn to obtain the dynamic ground pressure of the crawler walking mechanism, and the influence of track parameters on ground-specific pressure was studied in detail. Zhou [16] tested the reconfigurable wheel-crawler walking mechanism by using RecurDyn V9R3 software, the interaction of the grouser parameters was further clarified, and the regression equation of the traction force of the walking mechanism was obtained. Li [17] has proposed a composite chassis with a wheel-rail combination and conducted theoretical analysis and dynamic simulation analysis. The validity of the design was verified using RecurDyn, and the new chassis enhances the vehicle's ability to operate

under complex and diverse unstructured conditions. Hu [18] obtained the vertical load value of each track roller under typical working conditions and the overall pressure distribution in the track by computer simulation analysis. Pan [19] used the multi-body dynamics software to obtain the stress distribution of the track frame of the cone drill and the average load of the track roller. Wang et al. [20] established the dangerous working condition and obtained the load of the track roller under dangerous working conditions by conducting a dynamic simulation analysis of the mine excavator.

From the above literature search, it may be found that great progress has been made in the rail-wheel contact. However, many studies are primarily focused on trains [21,22] and small engineering vehicles [23,24], and few studies investigate large heavy-duty mining equipment. At the same time, although many scholars have conducted a large amount of work on the analysis of track roller, they focus on the static load, which neglects the load variation law of each track roller in actual working conditions. What’s more, in the study of the track roller, few scholars have studied the influencing factors of contact characteristics from the perspective of finite elements.

In order to study the complicated load characteristics of large mining machinery and the stress-changing law of the track roller, this paper is organized as follows. Section 2 establishes a mathematical model of the contact between the track roller and the track plate using the classical Hertz theory. Section 3 establishes a dynamic model of the crawler walking device and investigates the variation of vertical dynamic loads on the track rollers under typical working conditions of the spreader. In section 4, finite element analysis of the track roller is conducted and compared with the results from the Hertz theory to validate its accuracy. The influencing factors analysis of contact characteristics are presented in Section 5. Section 6 is devoted to the concluding remarks. The results in this paper can provide a reference for research on large mining machinery and the rational design of track rollers.

## 2.0 THEORETICAL MODEL OF MAXIMUM CONTACT PRESSURE

The three-dimensional model between the track roller and track plate is established as shown in Figure 4. Here, surface I represents the spatial rotational surface of the track roller, while surface II represents the track plate and  $r_1$  denotes its cylindrical surface radius.  $R_2$  is the radius of the roller rim, and  $R_1$  is the radius of the track roller.

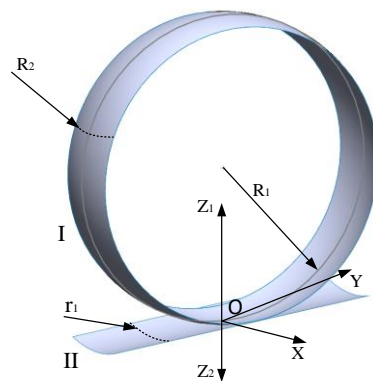


Figure 4. Contact model between the track roller and plate

Table 1. Contact stress calculation by Hertz theory

Nomenclature	Formula
Geometric constants	$A + B = \frac{1}{2} \left( \frac{1}{R_2} + \frac{1}{R_1} + \frac{1}{r_1} + \frac{1}{r_2} \right)$ $B - A = \frac{1}{2} \left[ \left( \frac{1}{R_2} - \frac{1}{R_1} \right)^2 + \left( \frac{1}{r_1} - \frac{1}{r_2} \right)^2 + 2 \left( \frac{1}{R_2} - \frac{1}{R_1} \right) \left( \frac{1}{r_1} - \frac{1}{r_2} \right) \cos 2\psi \right]^{\frac{1}{2}}$
Constants of materials	$k = \frac{1 - \nu^2}{\pi E}$ $\theta = \arccos \frac{B - A}{A + B}$
Auxiliary values	$m = 2.6250$ $n = 0.5047$
Semi-major radius of contact ellipse	$a = m^3 \sqrt{\frac{3\pi V k}{2(A + B)}}$

Table 1. (cont.)

Nomenclature	Formula
Semi-minor radius of contact ellipse	$b = n_3 \sqrt{\frac{3\pi V k}{2(A+B)}}$
Maximum contact pressure	$p = \frac{3V}{2\pi ab}$ ( $V$ : vertical load which is exerted on the track roller)

According to the Hertz theory of elastic contact, the maximum pressure in an ellipsoidal contact area could be obtained by the equations which are given in Table 1. In Table 1,  $\psi$  is the angle between the planes of maximum (or minimum) curvature,  $r_2$  is the track plate radius and it tends towards infinity.  $E$  denotes elastic modulus, and  $\nu$  is the Poisson's ratio of materials. At the same time, it could be seen that the maximum pressure at the center of a contact area is proportional to the vertical load, and it becomes smaller when the contact area between two bodies is larger. Therefore, the obtaining of accurate load is very important for the calculation of the maximum contact pressure.

### 3.0 VERTICAL DYNAMIC LOADS OF TRACK ROLLERS

In this paper, a certain type of spreader is taken as the research object, its main parameters are given in Table 2. In addition, the crawler walking device of the spreader is primarily composed of a driving wheel, track roller, riding wheel, guide wheel, track link, and track frame. In this paper, starting from the track roller closest to the driving wheel, the track rollers are numbered from 1 to 8 in sequence, as shown in Figure 5.

Table 2. Main parameters of the spreader

Parameter Category	Value
Mass of tracked vehicle (kg)	650 000
Track center distance (m)	10
Ground contact length of crawler (m)	8.60
Ground contact width of crawler (m)	2.70
Number of rollers	8×2
Track roller radius(mm)	275
Track roller rim radius(mm)	280
Track plate cylindrical surface radius(mm)	300
Driving wheel diameter(mm)	1600
Driving torque (kN·m)	1000
Maximum speed of driving wheel (rad·s <sup>-1</sup> )	0.16

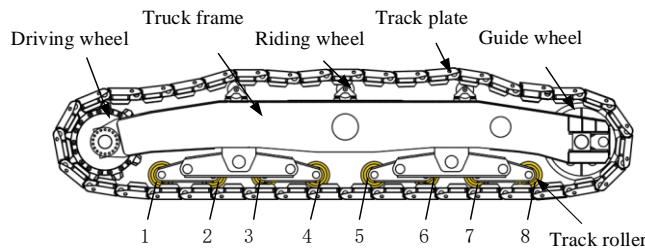


Figure 5. Structure diagram of the crawler walking device

A virtual prototype model of the crawler walking device is established and imported into RecurDyn as shown in Figure 6. Based on the actual walking process of the spreader, three typical operating conditions including running on a straight road, climbing a slope, and pivot steering are determined, as shown in Figure 7.

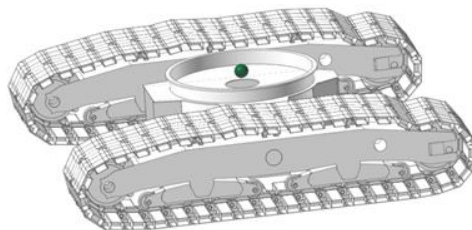


Figure 6. Virtual prototype model of crawler walking device

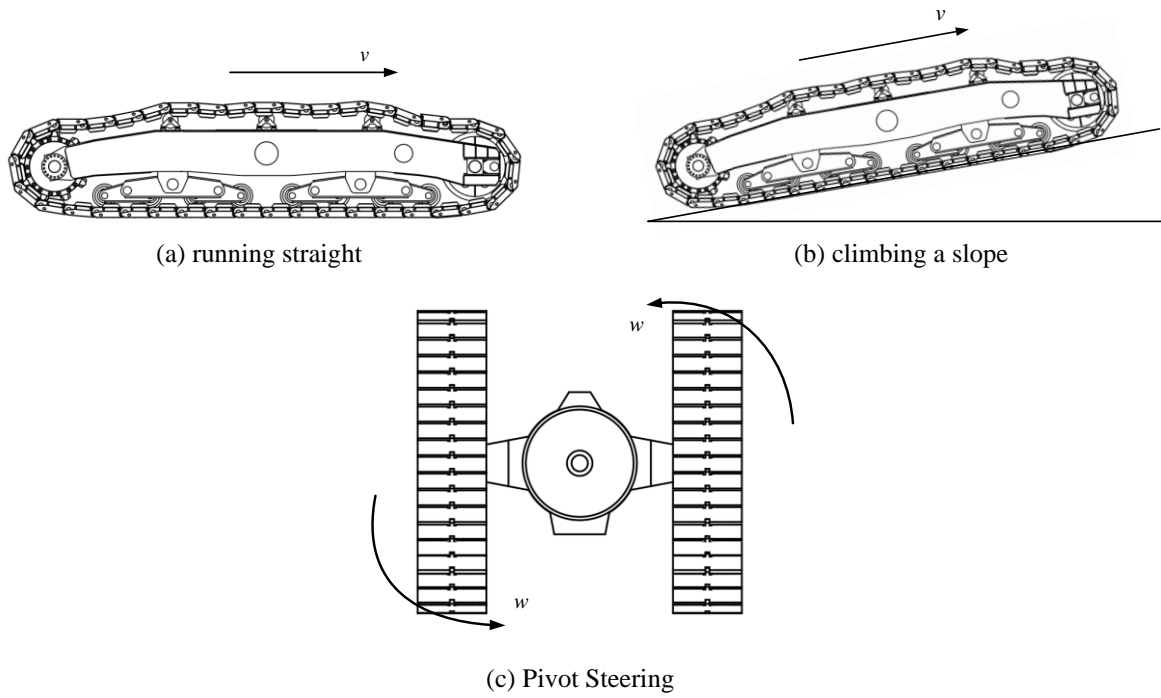


Figure 7. The diagram of typical working conditions

### 3.1 Running Straight

When the crawler vehicle runs on a straight road, the forces on the right and left tracks are the same [25]. At this time, the vertical load variation curves of each track roller on a single side are shown in Figure 8. From Figure 8, it can be observed that under the condition of running straight, the load changes of each track roller are different. The dynamic load on the first track roller varies from 151.89kN to 917.93kN, reaching a maximum value of 917.93kN at 3.4s. At the same time, the dynamic load on the eighth track roller fluctuates between 303.98kN and 869.65kN, reaching a maximum value of 869.65kN at 2.8s. The other track rollers 2 to 7 also exhibit similar patterns of variation but with smaller magnitudes compared to track rollers 1 and 8. The overall variation range for track rollers 2 to 7 is between 116.19kN and 720.83kN. The maximum load of 720.83kN occurs at 8.8s on track roller 3, which is smaller than the peaks of track rollers 1 and 8, reduced by 21.5% and 17.1% respectively. More importantly, the two sides of track rollers experience slightly greater forces compared to the track rollers in the middle.

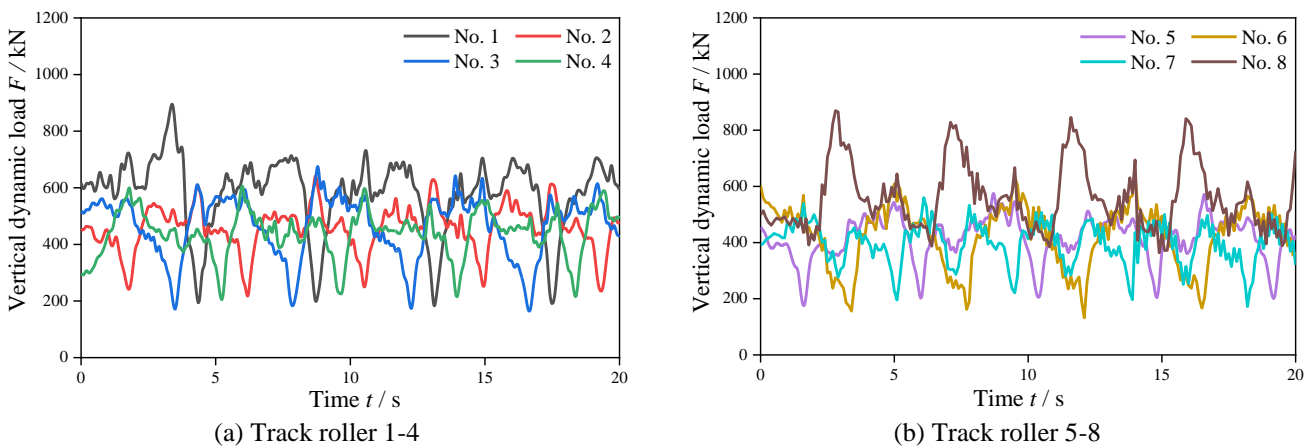


Figure 8. Loads of the track rollers under the running straight condition

### 3.2 Climbing a Slope

Similarly, When the crawler vehicle climbs on a slope, the forces on two tracks are also consistent. Therefore, the vertical loads of each track roller under this condition could be obtained, which are shown in Figure 9.

From Figure 9, it can be observed that when the spreader climbs a slope, the dynamic loads of track rollers 1 to 8 are similar to those of the running straight condition. Track rollers 1 and 8 experience the most prominent dynamic load variations, while track rollers 2 to 7 exhibit smaller variations. The dynamic load on track roller 1 varies between 187.23kN and 1191.44kN, while the dynamic load on track roller 8 changes from 271.79kN to 873.39kN. The maximum values of 1191.44kN and 873.39kN are reached at 3.1s and 15.7s, respectively. The overall variation range for track

rollers 2 to 7 is between 113.70kN and 712.26kN, with track roller 3 reaching its maximum load of 712.26kN at 17.2s. Compared with the running straight, the maximum loads of track rollers 1 and 8 increased by 22.9% and 0.4%, respectively. Throughout the above analysis, it may be found that track roller 1 experiences the maximum dynamic load, with a maximum value of 1191.44kN.

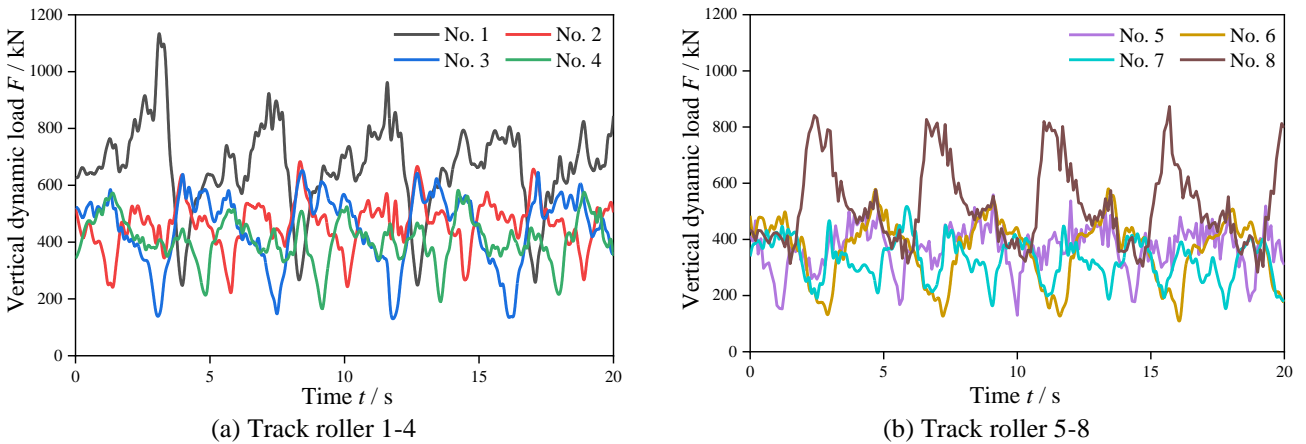


Figure 9. Vertical dynamic load of the track roller under climbing a slope

### 3.3 Pivot Steering

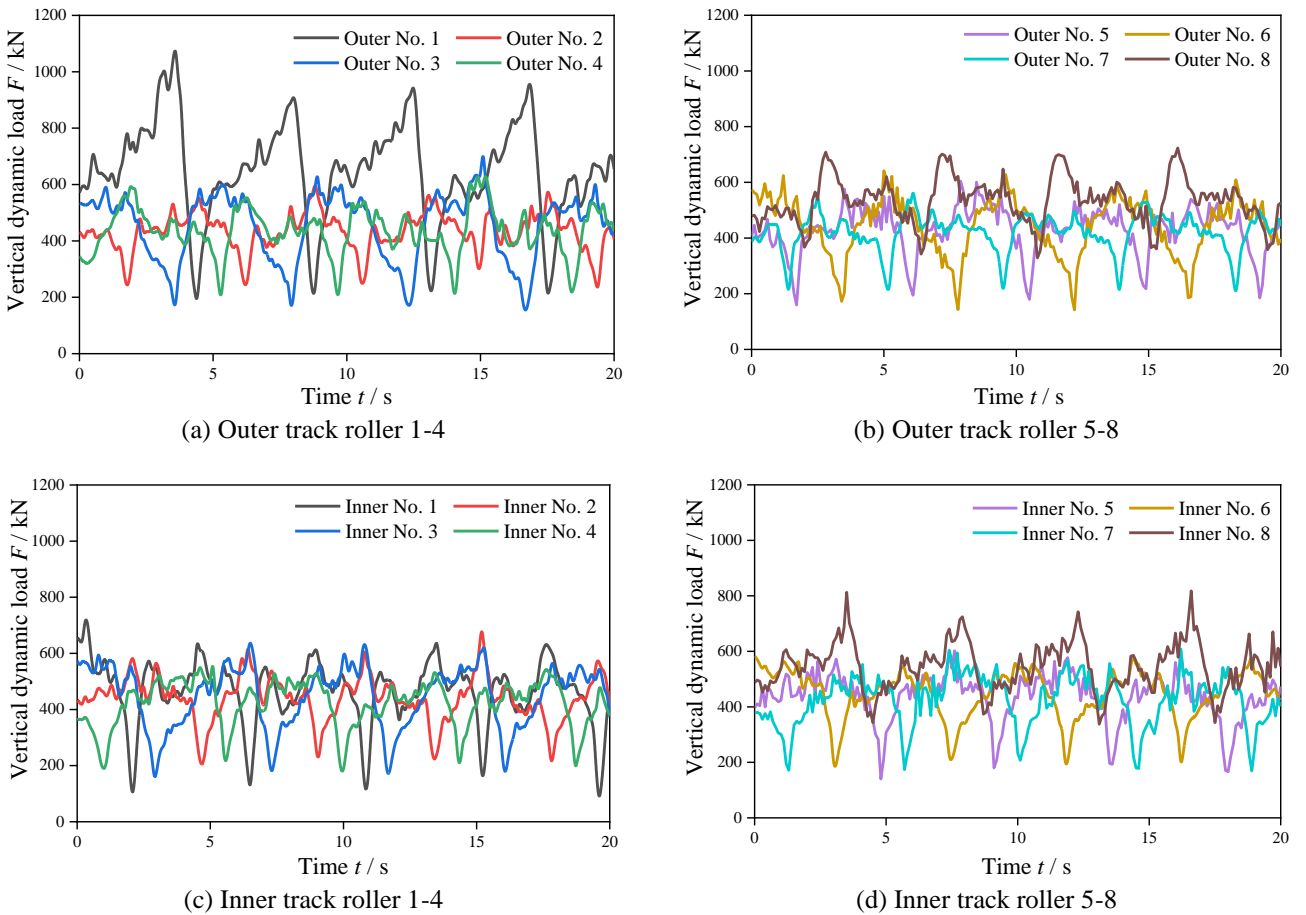


Figure 10. Vertical dynamic load of the track roller under steering condition

The pivot steering of tracked vehicles refers to a steering method in which the inner and outer track speeds are equal, but the driving wheels on both sides rotate in opposite directions. At this time, it is necessary to analyze the two tracks, and the load of the track roller of each track is shown in Figure 8.

From Figure 10, it can be seen that during the pivot steering condition, the dynamic load of the outer track rollers 1 to 8 fluctuates between 117.68kN and 1100.68kN, while the dynamic load of the inner track rollers 1 to 8 fluctuates between 62.2kN and 817.84kN. The maximum load on the outer track rollers occurs on track roller1 at 3.6s, reaching a maximum value of 1100.68kN. The maximum load on the inner track rollers occurs on track roller 8 at 16.6s, reaching a maximum value of 817.84kN. This indicates that the dynamic load variation is more remarkable on the outer track rollers. Compared

with the maximum loads during running straight, the maximum load on outer track roller 1 increased by 16.6%. Therefore, it could be known that the load of the outer track roller 1 is still the largest among all the loads under the condition of pivot steering.

Table 3. Maximum vertical dynamic load on the track roller under three different conditions

Number of track roller	Maximum vertical dynamic load / kN			
	Running straight	Climbing a slope	Pivot Steering	
			Inner	Outer
1	917.93	1191.44	733.78	1100.94
2	674.67	694.98	712.99	612.18
3	720.84	712.26	652.23	747.48
4	633.61	612.89	601.70	651.81
5	604.59	558.64	601.91	604.30
6	641.31	612.72	598.89	641.66
7	559.72	523.52	608.76	588.89
8	869.67	873.39	817.84	723.53

Through the above analysis, it can be observed that the track rollers experience a violent load with a maximum value of 1191.44kN occurring at the position of track roller 1 when the tracked vehicles climb a slope. These load variations will lead to failures such as insufficient intensity or fatigue damage of track rollers. For the convenience of the next analysis, the maximum vertical loads on each track roller under three different conditions are summarized in Table 3.

#### 4.0 FINITE ELEMENT MODEL ESTABLISHMENT AND VERIFICATION

In this section, a finite element (FE) contact model of the track roller with track plate is built using Solidworks and imported into Ansys Workbench, which is shown in Figure 11. Thus, the Mises stress and contact stress of the track rollers may be analyzed using Ansys Workbench. Because of the limitation of paper length, the authors only give the analysis results under the climbing a slope, which are shown in Figure 12. Figure 12(a) provides a more comprehensive stress distribution, whereas Figure 12(b) shows the distribution of contact stress of the track roller.

According to Figure 12(a), it can be observed that the Mises stress in the track roller exhibits a symmetrical distribution. The maximum Mises stress is located in the area where the edge of the track roller is in contact with the track plate, and it is near the rim of the roller, with a maximum value of 921.34Mpa. This aligns with the primary failure mode of the track roller, which is surface peeling, as observed in actual operating conditions. In addition, the distribution of contact stress, which is shown in Figure 12(b), forms an elliptical contact area. The maximum contact pressure is located at the center of the ellipse, with a maximum value of 1750.4 MPa.

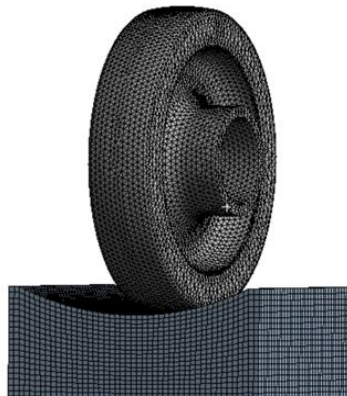


Figure 11. Finite element roller-plate contact model

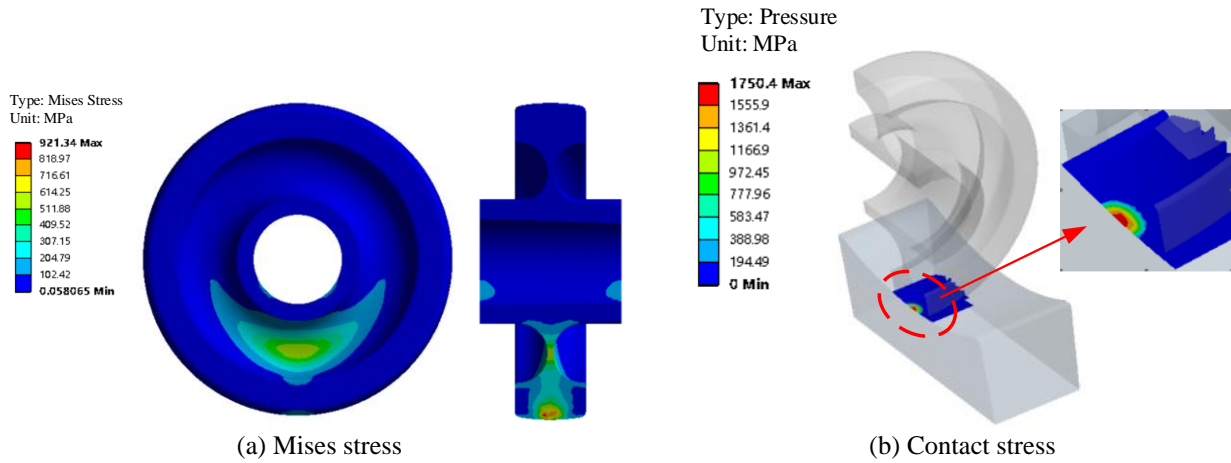


Figure 12. Stresses of climbing a slope

To further validate the accuracy of the finite element model, the maximum contact stress is calculated using the mathematical model established in Section 2. The comparison results are presented in Table 4. From Table 4, it could be found that the maximum error is 6.49%, and it is within a reasonable range. This demonstrates the validity of the model and the correctness of the simulation results.

Table 4. Comparison of Hertz contact theory and finite element

Typical conditions	Running straight	Climbing a slope	Pivot Steering
Hertz theoretical value / MPa	1544.86	1700.08	1658.88
FE simulation value / MPa	1652.00	1750.40	1725.20
Error between Hertz theory and FE	6.49%	2.87%	3.84%

In this study, the track roller and track plate are made of material G42CrMo4 with a yield strength of 930 MPa. According to reference [26], the permissible contact stress for high-strength alloy steel under point contact conditions is generally within 2000 MPa. Therefore, the strength of the track roller meets the usage requirements. However, both the maximum contact stress and Mises stress are approaching the critical permissible values. The track roller is highly susceptible to failure and damage when it works in such a load environment for a long period. Therefore, it is necessary to study the influence of relevant parameters on contact characteristics in order to extend the lifespan of the track roller.

### 5.0 INFLUENCING FACTORS ANALYSIS OF CONTACT CHARACTERISTICS

The contact stress between the track roller and plate is influenced by various factors, such as the vertical load, the radius of the track roller rim, the radius of the cylindrical surface of the track plate, and the used material, etc. Therefore, studying the impact of these factors on the contact stress between the roller and the track plate is of great significance for improving the roller-plate contact condition and extending the lifespan of the track roller.

#### 5.1 Vertical Load

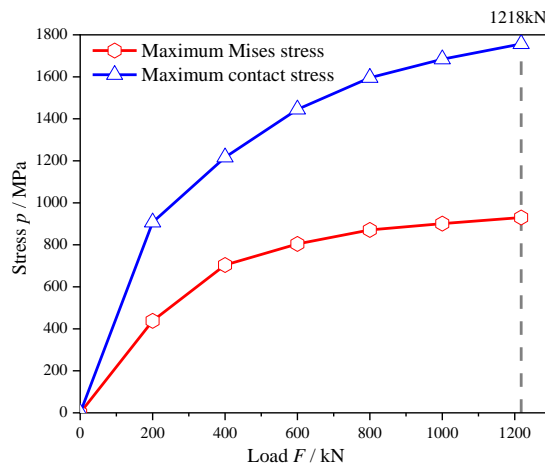


Figure 13. Contact characteristics variation with vertical load

Figure 13 illustrates the contact characteristics of the track roller under different vertical loads. It can be observed from Figure 13 that as the vertical load increases, both the maximum contact stress and maximum Mises stress of the track roller increase, but the rate of increase gradually decreases. When the load reaches 1218kN, the maximum Mises stress is 930.2MPa, and the maximum contact stress is 1756.5MPa, reaching the material's yield limit. If the load continues to increase, the track roller is highly susceptible to fatigue failure. Therefore, it is important to avoid excessive load in practical operations.

**5.2 Radius of the Track Roller Rim and the Cylindrical Surface of the Track Plate**

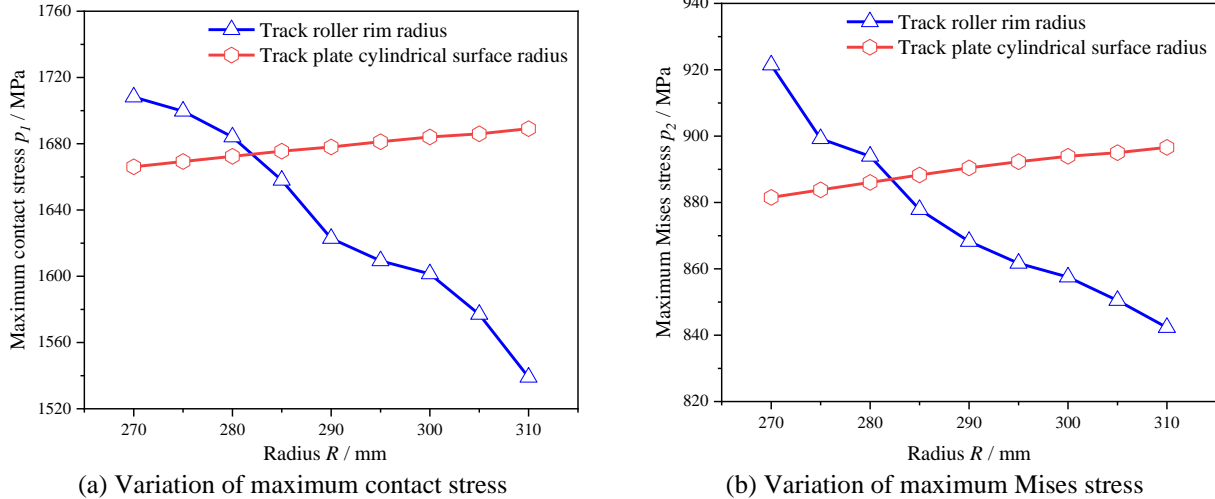


Figure 14. Variation of stress with the radius of the track roller rim and track plate cylindrical surface

During the operation of the tracked vehicle, the track roller may have transverse displacement or skew, resulting in the wear and deformation of the track roller and track plate. Therefore, the study of the influence of the rim radius of the track roller and the cylindrical radius of the track plate on the contact characteristics can better design and manufacture the track roller, to extend its service life.

An analysis was conducted with a vertical load of 1000kN on the track roller, and the results are shown in Figure 14. From Figure 14(a), it can be observed that as the track roller rim radius increases, the maximum contact stress gradually decreases. Conversely, as the track plate's cylindrical surface radius increases, the maximum contact stress gradually increases. From Figure 14(b), it is evident that the maximum Mises stress decreases gradually with an increase in the track roller rim radius, while it gradually increases with an increase in the track plate cylindrical surface radius. In conclusion, increasing the track roller rim radius and reducing the track plate cylindrical surface radius can decrease the contact stress and Mises stress, thereby improving the roller-plate contact conditions. In terms of stress variation amplitude, the influence of the track roller rim radius on the contact characteristics is more prominent.

**5.3 Material Property**

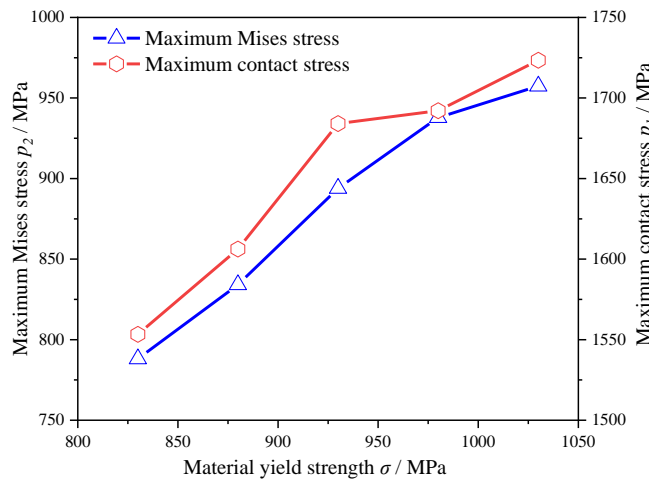


Figure 15. Variation of contact characteristics with yield strength of materials

The different heat treatment processes can alter the material yield strength of the track roller and track plate, which will influence the roller-plate contact characteristics. Assuming that the yield strengths of the track roller are 830MPa, 880MPa, 930MPa, 980MPa, and 1030MPa respectively, the effects of different yield strengths on the roller-plate contact characteristics are compared when the track roller is subjected to a vertical load of 1000kN. The results are shown in

Figure 15. From Figure 15, it could be known that as the yield strength of the track roller increases, both the maximum Mises stress and contact stress also increase. However, the maximum Mises stress consistently remains lower than the material's yield strength. In practical manufacturing processes, if the material yield strength of the track roller is increased, the hardness of the track roller would also increase, and this will lead to a higher risk of slippage. Simultaneously, it would also elevate the production cost of the track roller.

## 6.0 CONCLUSIONS

In this paper, the heavy-duty track roller of the spreader is taken as a research object. Using the multibody dynamics software RecurDyn, the load variations of the track roller during actual working processes were obtained. After that, Ansys Workbench was utilized to establish a finite element model for the contact analysis between the track roller and the track plate. The accuracy of the model and simulation results was verified using Hertz contact theory. Furthermore, the effects of various parameters on the roller-plate contact characteristics were investigated. The following conclusions are drawn:

- a) Under three typical operating conditions, the track rollers experience the largest load while climbing a slope, with a maximum load of 1191.44kN. Additionally, the load variation demonstrates that the two ends of track rollers experience greater loads compared with the other middle track rollers.
- b) The track roller experiences the biggest stress while climbing a slope, with a maximum Mises stress value of 921.34MPa. The maximum Mises stress is located in the area where the edge of the track roller is in contact with the track plate. The maximum contact stress value of 1750.4 MPa is located at the center of the contact ellipse.
- c) With the vertical load, track plate cylindrical surface radius, and material yield strength increases, both the maximum Mises stress and maximum contact stress also increase. However, as the track roller rim radius increases, the maximum Mises stress and maximum contact stress gradually decrease.

The results of this paper can provide theoretical support for the design of the spreader, and provide some reference for the structural improvement and parameter optimization of the track roller.

## 7.0 ACKNOWLEDGEMENT

The authors would like to thank the Key Research and Development Program of Shanxi Province (Grant No.202102010101010) and the Shanxi Province Postgraduate Education Innovation Project (2022Y672, 2023KY638) for their support.

## 8.0 REFERENCES

- [1] Y. Zhou, Dynamic Analysis of Statically Determinate Portal Structure of Double-Crawler Spreader. Master Thesis. Beijing: Tsinghua University, 2013.
- [2] P. L. Huo, Static and Dynamic Characteristics Analysis and Lightweight Research of Key Structure of Spreader. Master Thesis. Taiyuan: Taiyuan University of Science and Technology, 2021.
- [3] J. Arvidsson, H. Westlin, T. Keller and M. Cilbertsson. "Rubber track systems for conventional tractors—Effects on soil compaction and traction," *Soil and Tillage Research*, vol. 117, pp. 103-109, 2011.
- [4] T. Keller and J. Arvidsson, "A model for prediction of vertical stress distribution near the soil surface below rubber-tracked undercarriage systems fitted on agricultural vehicles," *Soil and Tillage Research*, vol. 155, pp. 116-123, 2016.
- [5] H. Hertz, "Über die Berührung fester elastischer Körper," *Journal für die reine und angewandte Mathematik*, vol. 1882, pp. 156-171, 1882.
- [6] W. Yan and F. D. Fischer, "Applicability of the Hertz contact theory to rail-wheel contact problems," *Archive of applied mechanics*, vol. 70, pp. 255-268, 2000.
- [7] G. Q. Tao, Z. F. Wen, X. Zhao and X. S. Jin, "Effects of wheel–rail contact modelling on wheel wear simulation," *Wear*, vol. 366, pp. 146-156, 2016.
- [8] H. Tian, Y. Fang, S. Wang, Z. R. Chen and C. L. Yan, "Analysis and Optimization of Static Contact Characteristics of Heavy-Duty Tracked Vehicle Rollers," *Mathematical Problems in Engineering*, vol. 2021, pp. 1-12, 2021.
- [9] M. R. Aalami, A. Anari, S. Torkan and S. Talatahari, "A robust finite element analysis of the rail-wheel rolling contact," *Advances in Mechanical Engineering*, vol. 5, p. 272350, 2013.
- [10] M. A. Arslan and K. Oğuz, "3-D Rail–Wheel contact analysis using FEA," *Advances in Engineering Software*, vol. 45, pp. 325-331, 2012.
- [11] P. K. Sen, M. Bhiwapurkar and S. P. Harsha, "Numerical Simulation and Parametric Analysis of Fatigue Crack in UIC60 Rail Thermite Welded Joint," *In: IOP Conference Series: Materials Science and Engineering*, vol. 1206, no. 1, p. 012027, 2021.
- [12] Z. H. Yan, G. Q. Wang, Z. W. Yao and H. T. Chen, "Contact Analysis on Huge Crawler Track Wheel and Track Pad," *Transactions of the Chinese Society of Agricultural Engineering*, vol. 28, pp. 51-56, 2012.
- [13] M. A. Arsić, S. M. Bošnjak, Z. D. Odanović, M.M. Dunjić, and A.M. Simonović "Analysis of the spreader track wheels premature damages," *Engineering Failure Analysis*, vol. 20, pp. 118-136, 2012.

- [14] G. G. Sirata, H. G. Lemu, K. Waclawiak, et al. "Study of rail-wheel contact problem by analytical and numerical approaches," *In: IOP Conference Series: Materials Science and Engineering*, vol. 1201, no. 1, p. 012035, 2021.
- [15] T. G. Pei, B. J. Yan, Z. K. Liu and Z. D. Zhao, "Dynamic ground pressure prediction of heavy-duty construction vehicles considering crawler parameters," *Journal of the Brazilian Society of Mechanical Sciences and Engineering*, vol. 45, p. 158, 2023.
- [16] P. Zhou, S. Tang and Z. Sun, "Simulation Research on the Grouser Effect of a Reconfigurable Wheel-Crawler Integrated Walking Mechanism Based on the Surface Response Method," *Applied Sciences*, vol. 13, p. 4202, 2023.
- [17] Y. Li, L. Zang, T. Shi, et al. "Design and dynamic simulation analysis of a wheel-track composite chassis based on RecurDyn," *World Electric Vehicle Journal*, vol. 13, p. 12, 2021.
- [18] Y. H. Hu, Dynamics Research on Travelling Mechanism of Crawler Mining Excavators. Master Thesis. Changchun: Jilin University, 2011.
- [19] T. Pan, Simulation Analysis and Optimization Research of Crawler Travelling Device of Rotary Drill Dig. Master Thesis. Changchun: Jilin University, 2017.
- [20] Y. B. Wang, X. H. Li, J. J. Ren, et al. "Dynamic Behavior Anlysis for Crawler Driving Mechanism of Mine Excavator," *Mining Research and Development*, vol. 38, pp. 119-123, 2018.
- [21] M. N. Tawfik, M. M. Padzi, S. Abdullah, et al. "A Review of the Rolling Contact Fatigue of Rail Wheels Under Various Stresses," *Journal of Failure Analysis and Prevention*, vol. 23, pp. 16-29, 2023.
- [22] S. Baltic and W. Daves, "Squat initiation mechanism model in a rail-wheel contact," *Engineering Fracture Mechanics*, vol. 269, p. 108525, 2022.
- [23] Isdhianto, Analisa Kerusakan dan Perbaikan Roller Pada Excavator XGMA XG822EL. Master Thesis. Surakarta: Universitas Muhammadiyah Surakarta, 2018.
- [24] H. Sun, Y. Zhou, X. Liao, et al. "Abrasive wear characteristics of 40Mn2 steel in simulated condition of sprocket wheel in crawler bulldozer walking system," *Surface Topography: Metrology and Properties*, vol. 7, p. 035012, 2019.
- [25] L. Y. Qing, Walking Performance Analysis and Track Shoe Structure Parameters Optimization of Tracked Vehicle. Mas Thesis. Xiangtan: Hunan University of Science and Technology, 2020.
- [26] X. Q. Yang, S. R. Liu and J. H. Cao, "Research on Yield Strength Problem of HERTZ Contact Stress," *Journal of Mechanical Strength*, vol. 38, pp. 580-584, 2016.